Chapter 2

Energy Transition Outlook and Best Available Technology

May 2022

This chapter should be cited as
ERIA Study team (2022), 'Energy Transition Outlook and Best Available Technologies', in Yamada, F., K. Murakami, H. Phoumin (eds.), *Study on Enhanced Flexibilisation of Coal-fired Power Plants for Optimal Grid Stabilisation in the ASEAN Region.* ERIA Research Project Report FY2022 No. 02, Jakarta: ERIA, pp.4-19.

Chapter 2
Energy Transition Outlook and Best Available Technologies

1. Outlook in the Energy Transition Period

ASEAN’s GDP growth in the coming 2 decades is projected to be one of the highest surges in the world (Figure 2.1, left). ASEAN’s GDP is projected to nearly triple from 2020 to 2040. Indonesia is the largest economic zone in ASEAN, followed by Malaysia, the Philippines, Thailand, and Viet Nam. In these expanding economies, electricity demand will remarkably increase (Figure 2.1, right). The energy policies in 2018, when the 6th ASEAN Energy Outlook (AEO6) was compiled, revealed that each country has no choice but to rely on fossil energy of coal- and gas-fired power. The renewable source is expected to play a critical role in the energy supply, simultaneously addressing climate change.

Figure 2.1. Projected ASEAN GDP Growth (left) and ASEAN Installed Capacity Growth (right) under AEO6

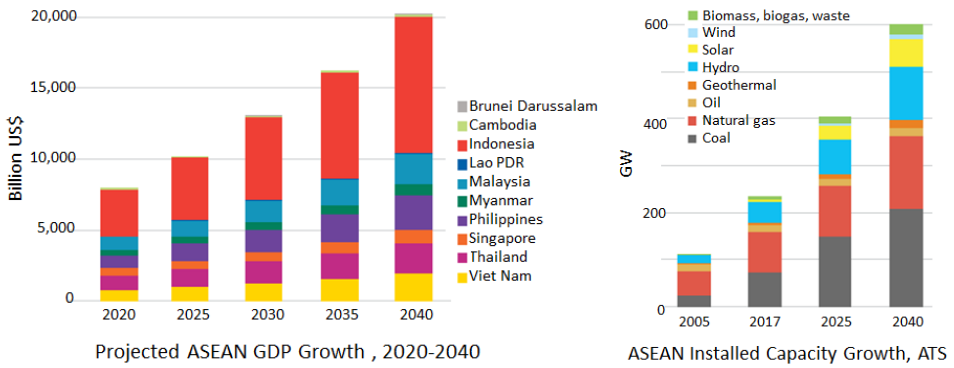

ATS = ASEAN Target Scenario.
Source: ASEAN Centre for Energy (2020).

Figure 2.2 shows the generation outlook of four countries based on the data from the AEO6. Despite the massive installation of renewable capacity, coal and gas energy is still the mainstay of power generation. In such a situation, grid fluctuation might occur by an un-optimised generation mix.

Each country aims for further carbon neutrality by adding renewable energy and reducing fossil energy, incorporating it into the latest power development plan. In such an energy transition, grid fluctuation might become severe if intermittent renewable energy, such as solar and wind, is introduced. Currently, this grid fluctuation issue should be addressed by all other energy sources connected to the same grid for further flexibilisation.

Figure 2.2. Generation Growth of ASEAN Target Scenario, 2020–2040

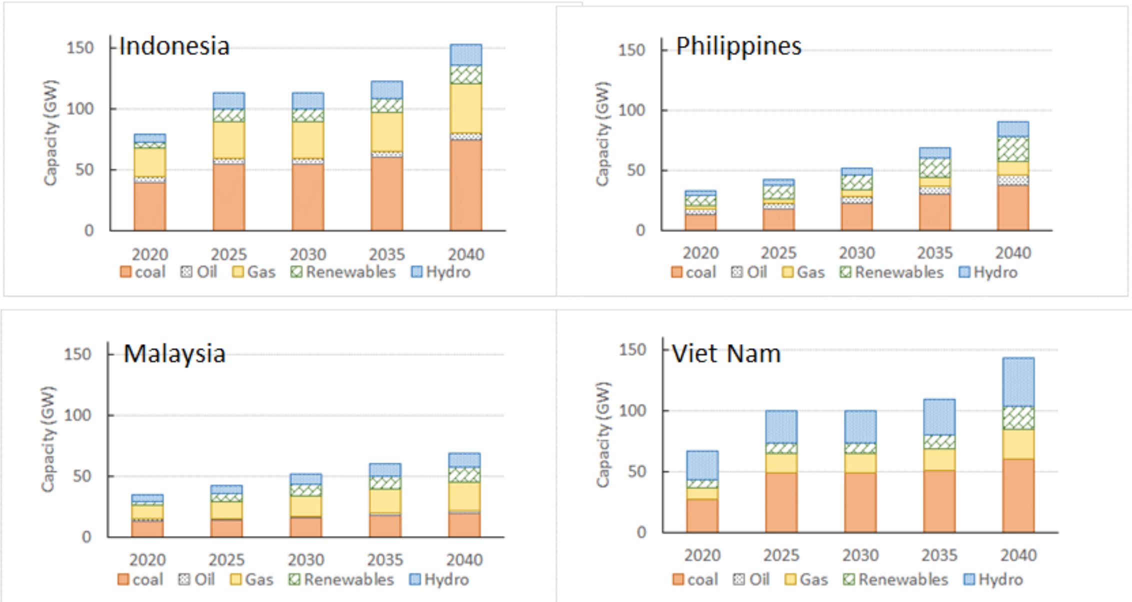

Source: ASEAN Centre for Energy (2020).

1.1. Grid Fluctuation Index (GFI) for preliminary analysis of future grid fluctuation

The daily variation curve of the energy demand is often shown as the 'Duck Curve' (Figure 2.3). The maximum ramp rate is to be a parameter showing the degree of grid fluctuation. But the value itself strongly depends on the grid size. The GFI is newly defined as a parameter to express the degree of grid fluctuation by calculating the maximum ramp rate and the total installed capacity of the grid.

Figure 2.3. Example of Duck Curve and Definition of GFI

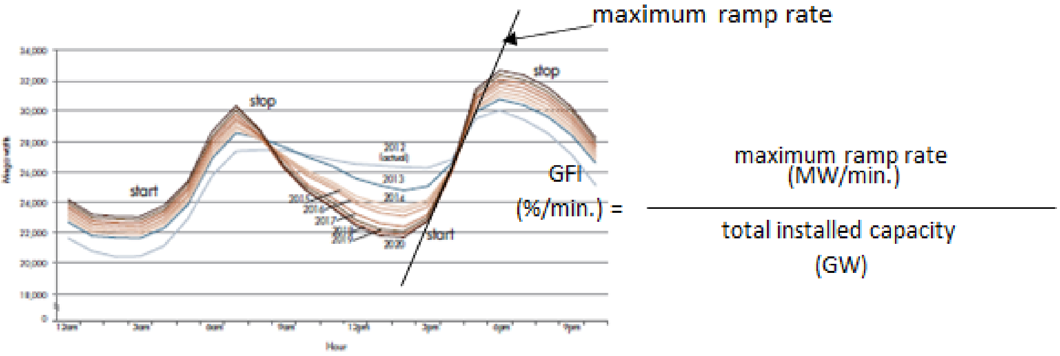

Source: Duck curve: [www.caiso](http://www.caiso.com).com.

Since such duck curves, especially future ones, are extremely limited to be obtained from the public domain, a GFI prediction formula was obtained by multivariate analysis from the limited data. Its details are described in the reference (IEC, 2021). The result of the GFI prediction formula is shown in formula (1):

$$GFI = w_1 X_{coal} + w_2 X_{nuclear} + w_3 X_{renew} + w_4 X_{solar} + E \quad (1)$$

where, X_{coal}, $X_{nuclear}$, X_{renew}, X_{solar} are energy availability factors of coal, nuclear, total renewables, solar, respectively; w_1, w_2, w_3, w_4 are coefficients for X_{coal}, $X_{nuclear}$, X_{renew}, X_{solar}, respectively; and E is a residual error of the regression.

Table 2.1. GFI Regression Model

X	Coefficient	Value
X_{coal}	w_1	0.0015
$X_{nuclear}$	w_2	-0.0001
X_{renew}	w_3	-0.0003
X_{solar}	w_4	0.0071
Residual error	E	-0.1258

Source: Authors' calculation.

The Q&A of GFI analysis in the 1st Working Group is in the Appendixes.

1.2. GFI behaviour of ASEAN, 2020–2040

Table 2.2 shows an estimated GFI of ASEAN by multivariate regression analysis.

Table 2.2. Estimated GFI of ASEAN Countries, 2020–2040

Country	2020	2025	2030	2035	2040
Brunei Darussalam	0.050	0.040	0.043	0.043	0.049
Cambodia	0.033	0.010	0.056	0.051	0.049
Indonesia	0.029	0.011	0.049	0.078	0.077
Lao PDR	0.000	0.000	0.000	0.000	0.000
Malaysia	0.088	0.095	0.095	0.095	0.096
Myanmar	0.035	0.000	0.028	0.047	0.061
Philippines	0.082	0.088	0.095	0.094	0.097
Singapore	0.021	0.012	0.007	0.000	0.000
Thailand	0.002	0.002	0.002	0.009	0.006
Viet Nam	0.059	0.025	0.070	0.103	0.098
ASEAN average	0.061	0.043	0.073	0.080	0.083

Source: IEC (2021).

The GFI of many countries – especially Indonesia, Malaysia, the Philippines, and Viet Nam – will remarkably increase from 2030. On the other hand, Singapore and Thailand seem to have less concern about grid fluctuation. Brunei, the Lao PDR, Cambodia, and Myanmar have relatively smaller grid sizes. There seems to be less concern about grid fluctuation. The grid scales of Indonesia, Viet Nam, the Philippines, and Malaysia are growing without any remarkable change in the power supply share; the grid fluctuation concern is likely to become apparent after 2030.

Figure 2.4. Estimated GFI Overview of ASEAN, by Year (left), by Coal Share (right)

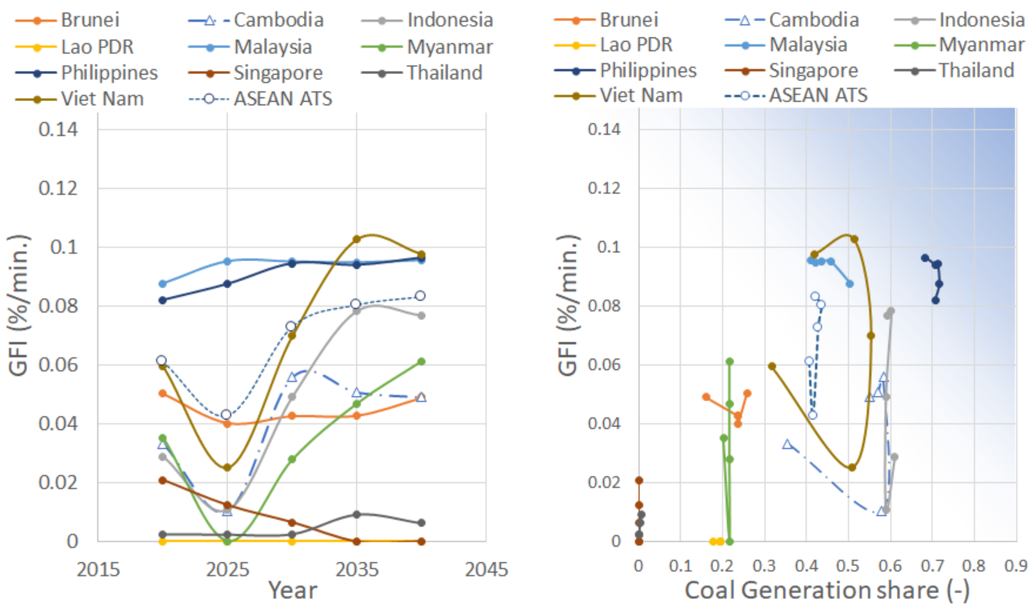

Source: IEC (2021).

Indonesia is projected to see its GFI surging after 2035. Flexibilisation with the CFPPs would be one major option to address the possible fluctuation of the national grid. The GFI of Malaysia will stay at a relatively high level at 0.09–0.1. Coal accounts for less than 50% of the generation mix. The GFI of the Philippines will remain at a relatively high level at approximately 0.08–0.1, which would require flexibilisation measures. High dependence on coal-fired power generation is deemed to be a major factor to expedite it. The local grid system fluctuation might occur more severely if the more flexible power supply sources such as gas and/or hydro are less available. The GFI of Viet Nam will stay relatively at a low level up to 2025, following which a sharp increase will be observed towards 2035. Installed capacity will continue to increase for the long term. As of 2040, coal will account for less than 40% of the generation mix. The ASEAN ATS in Figure is an average GFI of the ATS.

2. Key Resources and Technology for Grid Flexibilisation

This is an overview of the by-resource potential contribution to grid flexibility. All kinds of generations are plotted in this graph. Horizontal is a type of generation; vertical is generation capacity.

Figure 2.5. Overview of By-resource Potential Contribution to Grid Flexibility

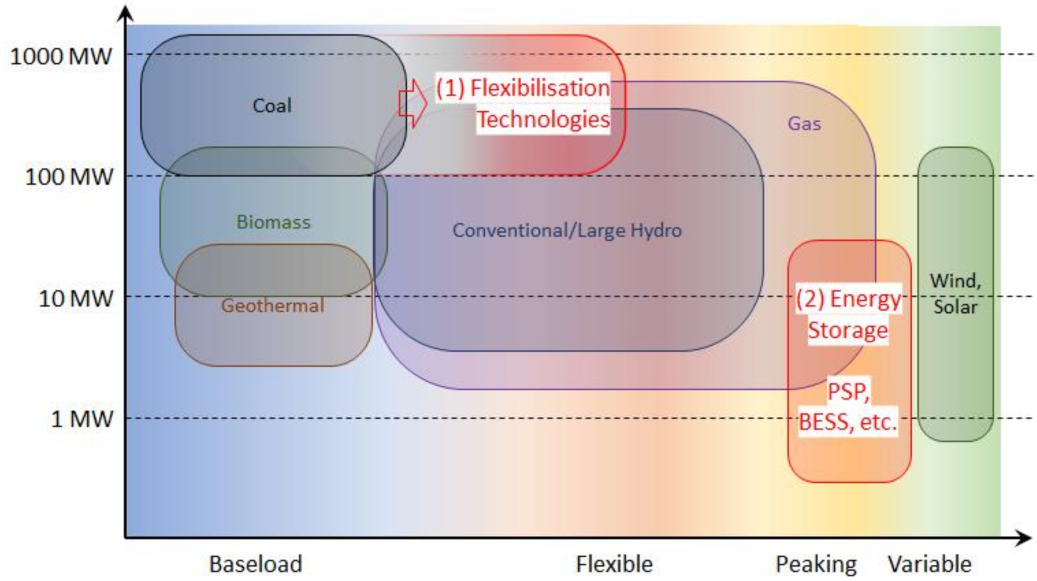

Source: Authors' calculation.

Coal and biomass generation is normally operated as baseload generation. Conventional large hydro and gas are operated widely from the baseload, flexible to peaking. Wind and solar are operated as intermittent variable renewable energy (VRE), the main reason for future grid fluctuation. Two major technologies are considered flexibilisation measures: technologies of CFPPs and energy storage, such as pump storage power (PSP) and battery energy storage system (BESS), etc.

2.1. Technical measures at the CFPPs

There are six key points in the flexibilisation technology of CFPPs: (i) improving loading rate, (ii) optimising minimum load, (iii) reducing start-up time, (iv) reducing life consumption, (v) Improving the control system, and (vi) modifying existing plants.

The first three key points are especially important. Figure 2.6 shows the three key points of the flexibilisation technology of CFPPs.

Figure 2.6. Three Key Points of Flexibilisation Technology

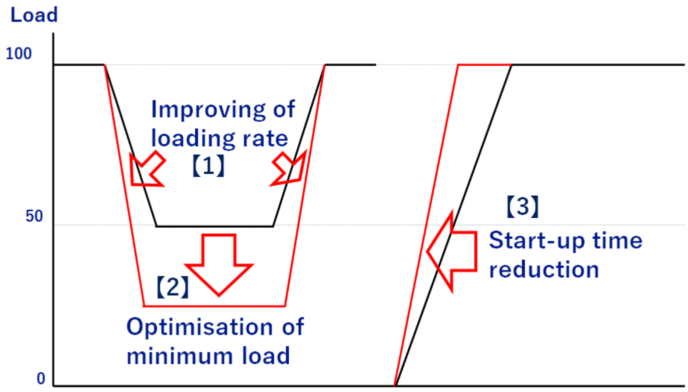

Source: Authors' calculation.

The most important factor in regulating the load of CFPPs is to improve the rate of load change. The first is improving the burning characteristics of coal. There are various types of mill pulverisers in CFPPs. Figure 2.7 shows the vertical mill pulveriser and the ball mill pulveriser. The second is improving steam temperature controllability.

Figure 2.8 shows an example of the main flow diagram. The third is the appropriate capacity of accessories, such as pulverisers, fans, pumps, and valves, and advancement of control equipment for steam temperature control. By introducing these, the load change rate can be improved from 3%/min to 5%/min.

Figure 2.7. Vertical and Ball Mill Pulverisers

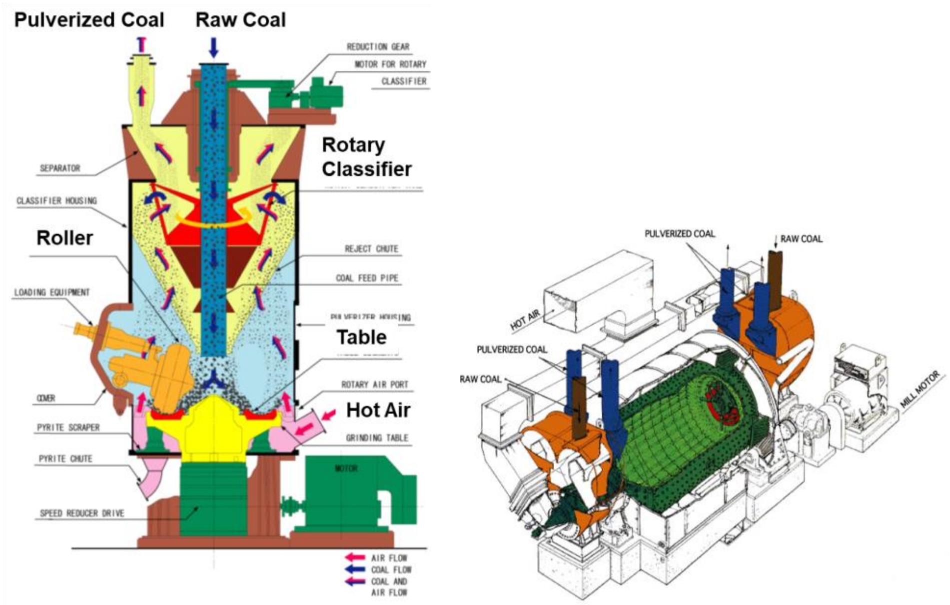

Source: Edited by JCOAL Original data from IHI.

Figure 2.8. Example of Main Flow Diagram

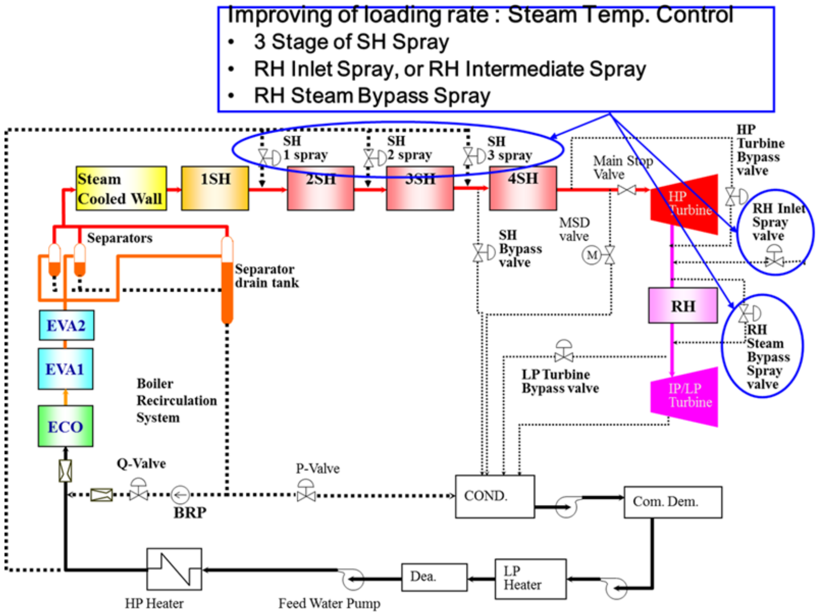

Source: Authors' calculation.

The next important point is optimisation of the minimum load. When the mill pulveriser is at low load, the pulverised coal at the outlet of the mill pulveriser is excessively lean as the air ratio is too high against coal. In this case, coal or oil must be increased to reach stoichiometric air–fuel ratio. Conventionally, the minimum load of coal-firing without oil support is limited to 30%–50% load. Figure 2.9 shows an example of a wide range burner (WRB) and burner turndown. The concentration ring is installed in the WRB. The figure on the right is an example of a burner turndown. The figure above is for a normal burner and the figure below is for a WRB. In the case of the WRB, the minimum load of coal firing without oil support is about 15%.

Figure 2.9. Wide Range Burner and Burner Turndown

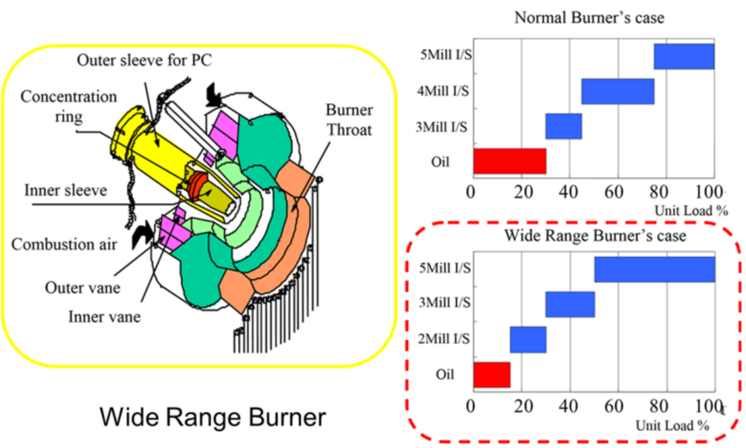

Source: Edited by JCOAL Original data from IHI.

The next third important point is reducing the start-up time. To shorten the start-up time, it is important to raise the turbine inlet steam temperature quickly. To that end, installing the following start-up bypass system, SH (super heater) bypass system, and high pressure/low pressure (HP/LP) turbine bypass system with RH (reheater) cooling or turbine bypass system without RH cooling. This start-up bypass system reduces the start-up time from ignition to full load from 120 minutes to 180 minutes. Figure 2.10 shows an example of a start-up bypass system diagram.

Figure 2.10. Example of a Start-up Bypass System Diagram

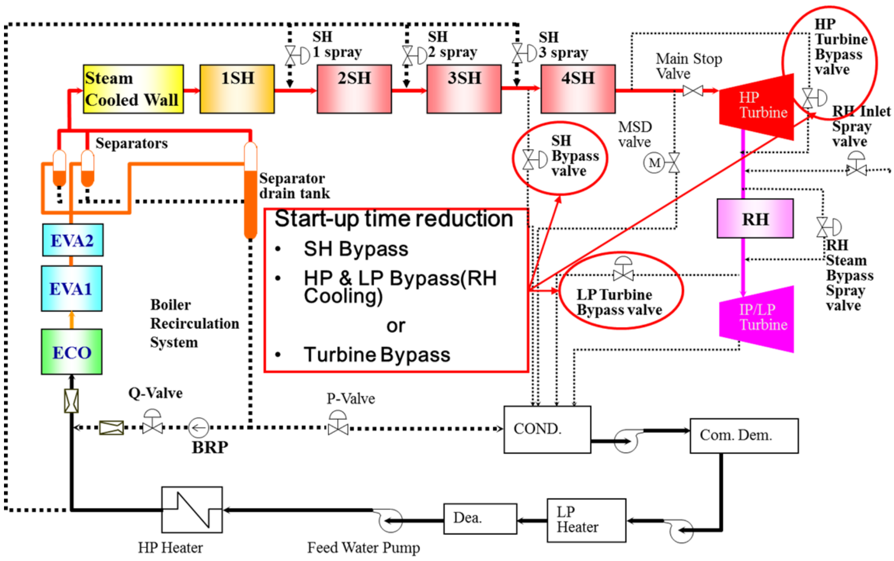

Source: Authors' calculation.

The improvement of the load change rate and the shortening of the start-up time lead to increased life consumption of the thick heat transfer part of the boiler. Here, the example of the reduction measures of the life consumption of the thick part of the boiler heat transfer part is introduced. Figure 2.11 shows some examples of the configuration of the heat transfer surface to minimise the thermal stress of the high-temperature parts. The upper left is the configuration of the heat transfer surface of the base, using the T piece. The upper right does not use the T piece; it adopts the end connection. The lower left is an example of adopting the end connection, splitting the heat transfer surface, and adding a spray between them. The lower right corner is an example that further improves by dividing the heat transfer surface in the furnace width direction.

Figure 2.11. Examples of Configuration of the Heat Transfer Surface

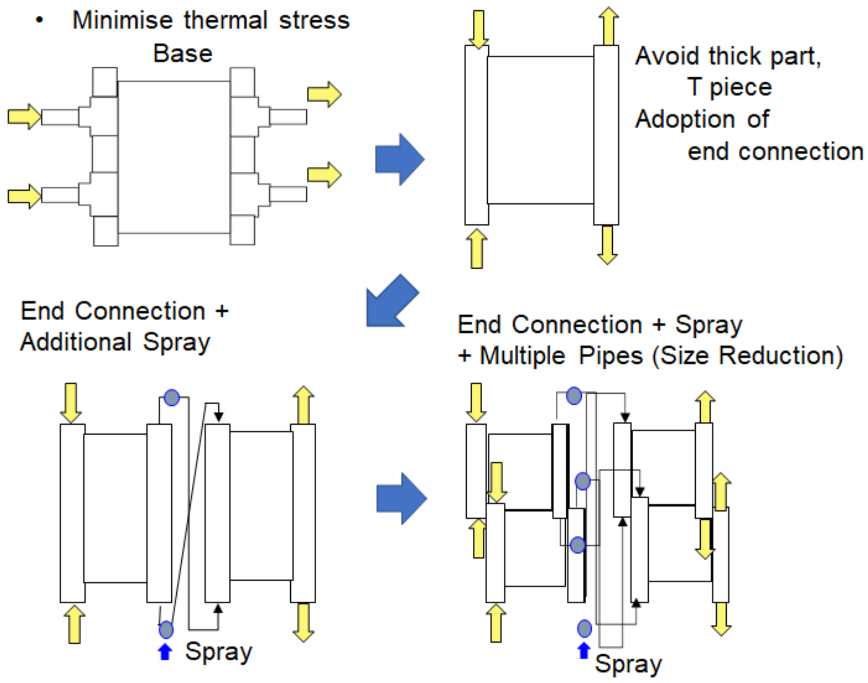

Source: Authors' calculation.

To improve the load adjustment function, it is important not only to improve equipment and systems but also to improve the control device and optimise the adjustment.

The operation ability improvement in the existing plant is explained. In the case of existing plants, it is important to clarify the purpose of functional improvement and comprehensively examine and remodel two small areas such as goals, effects, costs, and remodelling periods.

Some examples of remodelling existing plants are shown below.

- Modification of combustion equipment for a low load operation
- Number of mills: 1 mill, 2 mills, or all mills
- Number of burners: 1 row or 2 rows of burners, or all burners
- Improvement of steam temperature control
- Addition of SH spray 1 stage
- Reduction of start-up time
- Capacity increase of start-up bypass system

The following are examples of CFPPs in Japan that adopted WRBs.

Table 2.3. Examples of Adoption of Wide Range Burners (WRBs)

MW	No. of Mills	No. of Burners	No. of Mills that Adopted WRBs	No. of WRBs
33	2	8	1	4
250	4	24	2	8
600	6	36	2 → 6	12 → 36
700	6	36	6	36

Source: Authors' calculation.

2.2. Energy storage

Figure 2.12 shows the categories of energy storage technologies; horizontal is the module size and vertical is the discharge response. Pumped hydropower storage is plotted at the top right area, which means a moderate response and larger size. Compressed air and cryogenic energy are relatively smaller in size than the PSP. Several types of BESS, shown in blue, are positioned in the middle size and response. Especially, lithium-ion is now expanding its share each year globally because of its high energy densities.

Figure 2.12. Categories of Energy Storage Technologies

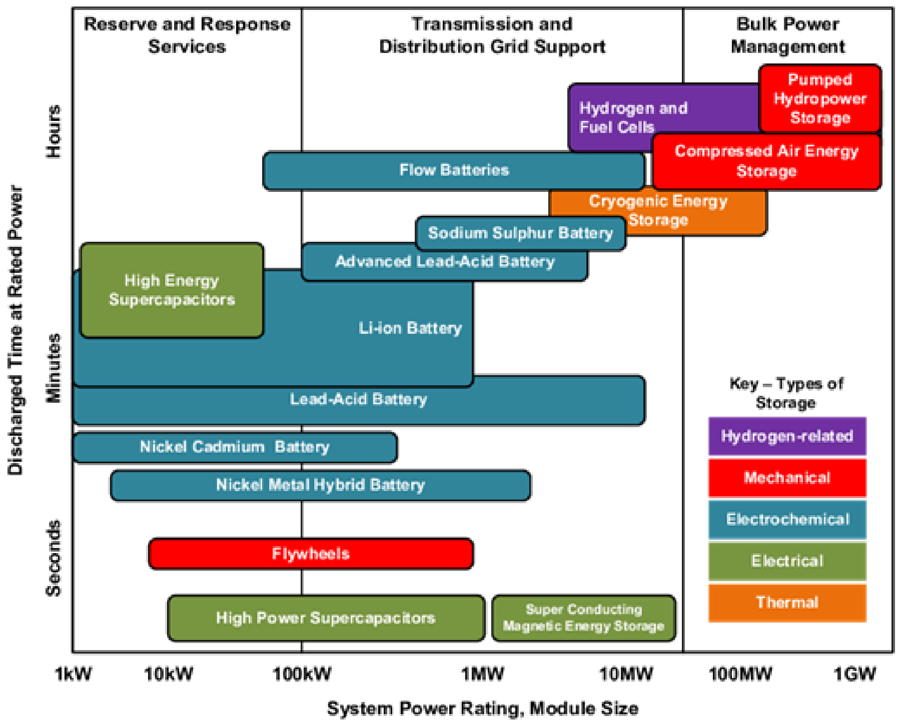

Source: Sprake et al. (2017).

Regarding quick response, high energy supercapacitor and superconducting magnetic energy device are shown. These kinds of technology are mainly used for uninterruptable power supply. BESSs of smaller size are normally used for ancillary support. According to this category, PSP, compressed air, and BESS are considered flexibilisation measures in this study.

Figure 2.13. Energy Storage Capacity in Japan

(GWh/y, GWh)	2020	2035
PSP	6800	6800
BESS	8	54.4

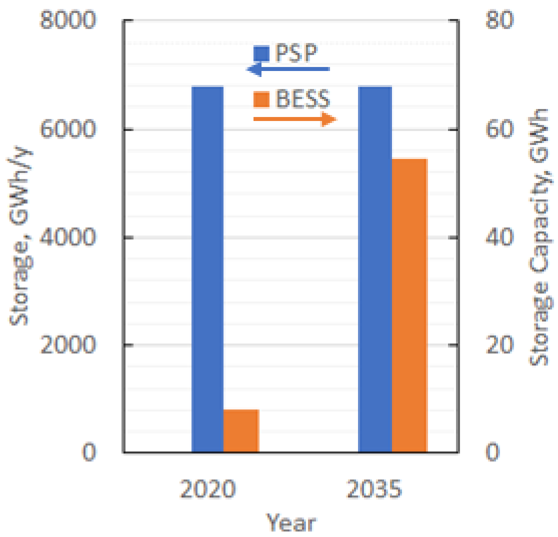

Source: Edited by JCOAL.

Figure 2.13 shows the energy storage capacity in Japan. Currently, PSP is the main energy storage; its annual energy storage is about 6.7 TWh/year. Since further suitable site situations for the PSP plant are limited, PSP is not expected to increase. On the other hand, mainly lithium-ion type BESS is drastically increasing.

Table 2.4 summarises the three main kinds of large energy storage technologies. Various electric energy conversions to potential, compressed, and electrochemical are currently available. PSP is a kind of potential energy. Small hydro can be easily converted to this type by renovating the turbine and generator with an additional pump function. The second is compressed energy. The energy charge is done by an electric power–driven pump up to the upper reservoir. Liquid air storage is an application of compressed energy. Charge–discharge is done by a simple mechanical operation of well-proven facilities and heat exchange without AD-DA conversion. The application of electrochemical energy is normally known as BESS. In this system, three technologies are suitable for large-scale energy storage: lithium-ion, sodium-sulphur, and redox flow batteries.

Table 2.4. Available Energy Storage Technologies

Technologies	Features	
Potential energy Pumped storage power	Pumped storage stores and generates energy by moving water between two reservoirs at different elevations. Excess energy is used to pump water to an upper reservoir at times of low electricity demand, like at night or on weekends,.	
Compressed energy Liquid air energy storage	The liquified air is converted back into pressurised gas, which drives turbines to produce electricity. Cost-effective supply–demand balancing besides ancillary services, such as grid stability, inertia, and reactive power	
Electrochemical energy Lithium-ion	Lithium-ion batteries are suitable for storing high-capacity power. They are used in various applications, including consumer electronics such as smartphones and personal computers, industrial robots, production equipment, and automobiles.	
Electrochemical energy Sodium Sulphur (NAS)	NAS battery is a high-temperature battery. Full discharge (SOC 100% to 0%) is available without capacity degradation. No self-discharge. Best performed with a long-duration application.	
Electrochemical energy Redox flow	Redox flow batteries are rechargeable batteries that are charged and discharged through the oxidation–reduction reaction of ions of vanadium or the like. The batteries are expected to serve as a technology to stabilise the power grids needed to expand the introduction of renewable energy, including solar and wind power.	

Source: Company websites: Toshiba Energy Systems & Solutions, https://www.toshiba-energy.com/en/renewable-energy/product/index.htm; Sumitomo Heavy Industries, Ltd., https://www.shi.co.jp/english/products/energy/cryobattery/index.html; NGK Insulators, Ltd. Sumitomo Electric Industries, Ltd., https://www.ngk-insulators.com/en/product/nas-solutions.html.

Figure 2.14. Pumped Storage Power

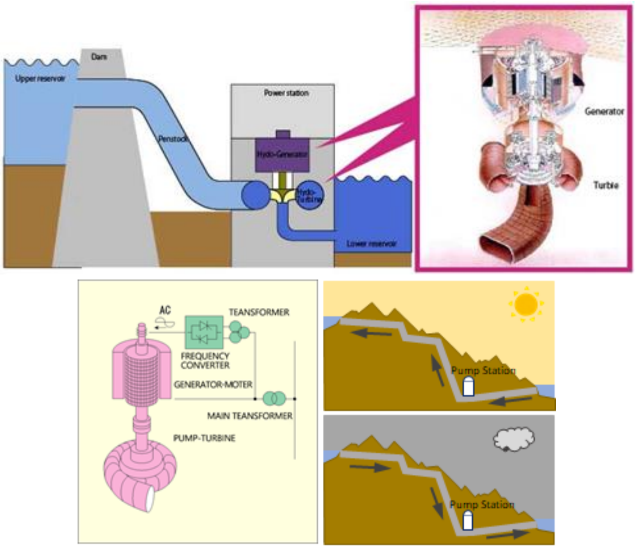

Source: Toshiba Energy Systems & Solutions website, https://www.toshiba-energy.com/en/renewable-energy/product/index.htm (accessed 1 October 2021).

Figure 2.14 shows a typical PSP system and water stream in charge and discharge.

'Adjustable-speed' PSP generation is mainly applied in Japan. The features of this technology are the following:

- Automatic frequency adjustment function during pumping operations
- Higher efficiency and expanded operation range during both generating and pumping operations
- Improved power grid stability
- Functions for maintaining the grid voltage.

Liquid air energy storage (LAES) technology (Figure 2.15) uses a freely available resource, air, cooled and stored as a liquid. As the discharging part, the liquified air is converted back into pressurised gas, which drives turbines to produce electricity. Air used for the driving turbine is recycled as an energy transfer medium with heat exchange at the charging part. LAES is ideal for replacing fossil fuel–based power plants by providing long-duration storage in renewable power systems. It offers cost-effective supply–demand balancing besides ancillary services, such as grid stability, inertia, and reactive power.

Figure 2.15. Liquid Air Energy Storage

Source: Sumitomo Heavy Industries, Ltd. website, https://www.shi.co.jp/english/products/energy/cryobattery/index.html (accessed 1 October 2021).

Figure 2.16 shows the three kinds of BESSs; these are demonstrated in major Japanese electricity utilities through governmental support. At the left is lithium-ion of 40 MWh; at the centre is sodium sulphur of 300 MWh; at right is a redox flow system of 60 MWh. Table 2.5 lists the typical performance of these three types. Lithium-ion has the highest energy density, making it the most advantageous to be developed and commercialised. That is why we use lithium-ion from mobile to vehicle in such large-scale energy storage.

Figure 2.16. BESS with a Wide Range of Choices

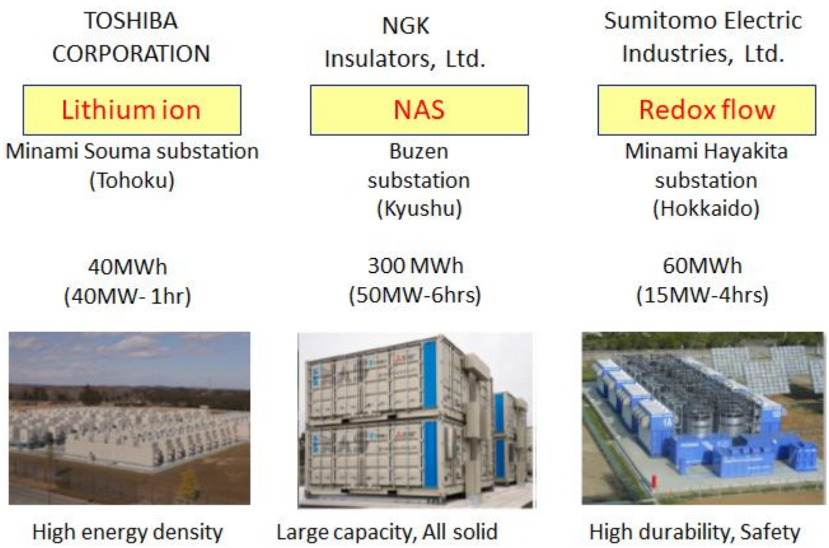

Source: Kyushu Electric Power, http://www.kyuden.co.jp/press_h160303-1_smt.html; Tohoku. Electric Power, https://www.tohoku-epco.co.jp/pastnews/normal/1191223_1049.html; Hokkaido Electric Power, https://www.hepco.co.jp/network/renewable_energy/efforts/large_accumulator/index.html.

Sodium-sulphur battery is initially developed for industrial applications to back up energy and uninterrupted power supply. Redox flow battery, most recently developed in Japan, uses metal ion reactions at room temperature. This technology has the advantage of long duration, and its capacity is easy to expand, only expanding the tanks of metal iron solution.

Table 2.5 Typical Performance of BESS

	Lithium Ion	Sodium Sulphur	Redox Flow
Cell voltage (V)	2.4–3.6	2.1	1.2–2.1
Energy density (W/kg)	70–200	100–130	10–30
Charge/discharge cycle	1,000 <	2,500–4,500	10,000 <

Source: Electric Power, http://www.kyuden.co.jp/press_h160303-1_smt.html; Tohoku. Electric Power, https://www.tohoku-epco.co.jp/pastnews/normal/1191223_1049.html; Hokkaido Electric Power, https://www.hepco.co.jp/network/renewable_energy/efforts/large_accumulator/index.html.

Examples of the commercial application of each BESS are shown in Figure 2.17, Figure 2.18, and Figure 2.19. All technology suppliers are now tackling system cost reduction and improvement of durability for expanding the global commercial network.

Figure 2.17. BESS Application by Toshiba

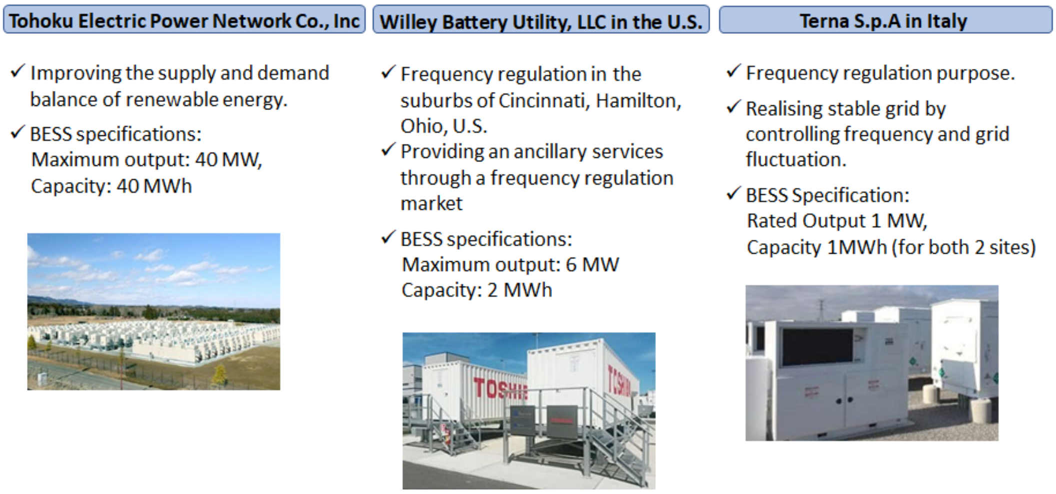

Source: Toshiba Corporation, https://www.global.toshiba/jp/products-solutions/battery/scib/application/power-system.html (accessed 1 October 2021).

Figure 2.18. BESS Application by NGK Insulators

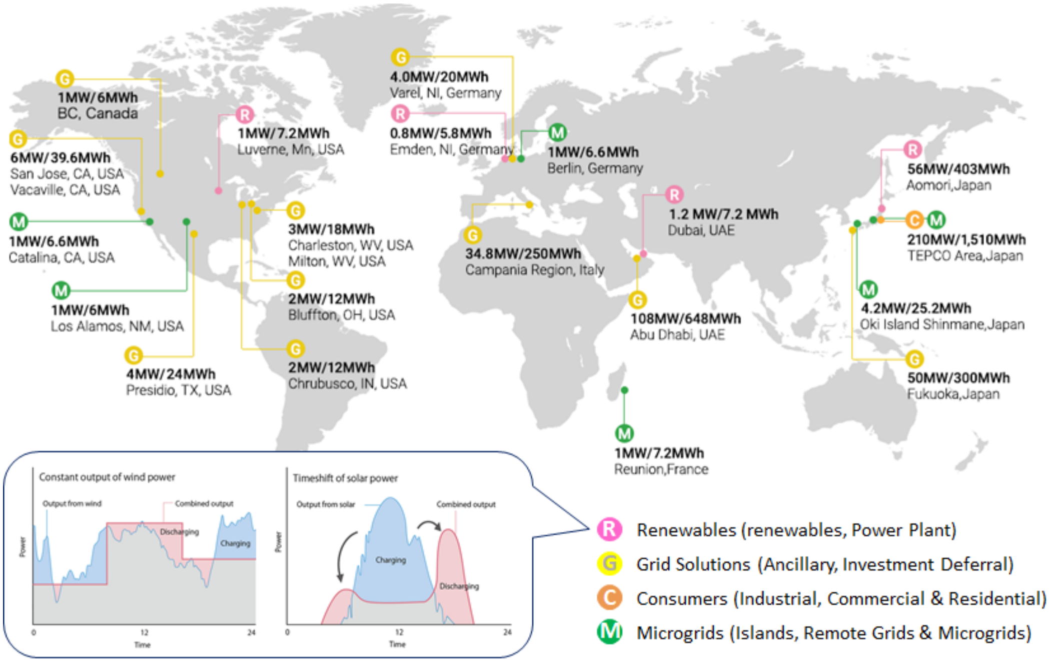

Source: NGK Insulators, Ltd., https://www.ngk-insulators.com/en/product/nas-solutions.html (accessed 1 October 2021).

Figure 2.19. BESS Application by Sumitomo Electric Industries

Source: Sumitomo Electric Industries, Ltd., https://sumitomoelectric.com/sites/default/files/2021-04/download_documents/Redox_Flow_Battery_En.pdf (accessed 1 October 2021).